UDC 551.509.313(215-13)

Southern Hemisphere Prediction Experiment With a Nine-Level, Primitive-Equation Model

REGINALD H. CLARKE—*Division of Atmospheric Physics, Commonwealth Scientific and Industrial Research Organization, Aspendale, Victoria, Australia*

ROBERT F. STRICKLER—*Geophysical Fluid Dynamics Laboratory,[1] NOAA, Princeton, N.J.*

ABSTRACT—A nine-level hemispheric primitive-equation model is applied to make a 14-day experimental prediction for the Southern Hemisphere; this is the first numerical prediction on the hemispheric scale for the Southern Hemisphere and the first attempt to use the model for summertime forecasting.

The predictions are verified against hemispheric data, the inadequacy of which is clear. They are also verified in the Australasian sector where the data are more adequate.

For the first 2 days, especially over areas with good data, the forecasts were generally of high quality, decreasing in accuracy with height above the surface. After a serious decline in skill on the fourth day, a recovery is noted. Australian rainfall during the first 2 days was also predicted with useful skill.

Some properties of the model atmosphere are compared with those of the observed Southern Hemisphere atmosphere, and deficiencies in the performance of the model, as well as in the analysis and initialization, are brought out by the comparison. However, on the whole, good agreement is found.

1. INTRODUCTION

The nine-level primitive-equation hemispheric general circulation model constructed by staff members of the Geophysical Fluid Dynamics Laboratory (GFDL), NOAA (Smagorinsky et al. 1965, Manabe et al. 1965), was used by Smagorinsky et al. (1967) and Miyakoda et al. (1969) for a series of Northern Hemisphere experimental forecasts.

Following the success of these experiments, we decided to gather data to enable us to make global forecasts as well as to separate hemispheric forecasts for comparison. Results of the global experiments are reported by Miyakoda et al. (1971*a*). The results of the hemispheric forecasts for the Southern Hemisphere are reported in this paper.

The present series of experiments, run in 1966, represents the first prediction experiments to be made on the hemispheric scale for the Southern Hemisphere and the first time the GFDL model has been applied to what is virtually a summer situation. Earlier modeling work had been reported (e.g., Jenssen and Radok 1960) for a restricted area. Other Southern Hemisphere forecasts of shorter time period have been made recently with less complex models (Baumhefner 1970, Staff, NMC 1970, Gauntlett and Hincksman 1971).

Such experiments are of interest for several reasons. They are useful, for example, to the contemporary Southern Hemisphere meteorologist when he considers the question of cost–benefit of improving data acquisition systems.

[1] At Forrestal Campus of Princeton University.

2. PREPARATION OF THE DATA

The starting time (0000 GMT on Mar. 1, 1965) for the experiments was chosen for the availability of satellite data from TIROS 9, both for initialization and verification. We hoped to use these data partly to overcome difficulties due to the sparseness of conventional data in the Southern Hemisphere. These difficulties are very real. In 1965, there were 85 daily radiosonde observations, less than 20 percent of the daily total in the other hemisphere, and these were mainly concentrated in Australasia (35), Antarctica (13), and South America (12). Figure 1, compiled from data available over the period Mar. 1–5, 1965, shows the mean number of data items per day at various heights and latitudes. (All available surface data were used, but only those from aerological stations are included in the figure.) One sees that, on the generous assumption that a daily sounding serves an area $10°\times10°$, in the troposphere the hemisphere is less than 30 percent covered by conventional observations. In the stratosphere, the coverage falls off to about 10 percent at 20 mb and is negligible at 10 mb. The data coverage is extremely poor in the 50°–60°S latitude belt, where the cyclonic centers most frequently occur (Taljaard 1967, Streten 1969). Figure 3B shows the location of data available at 500 mb on the initial day.

Construction of geopotential and temperature isopleths for the 1000-, 850-, 700-, 500-, 300-, 200-, 100-, 50-, 20-, and 10-mb levels proceeded by standard methods (differential analysis from the surface upward) where the data coverage is best. Over the blank areas, experience and audacity gained during years of Southern Ocean analysis (Clarke 1954) were used to project surface and 500-mb systems. Cloud photograph mosaics and nephanalyses

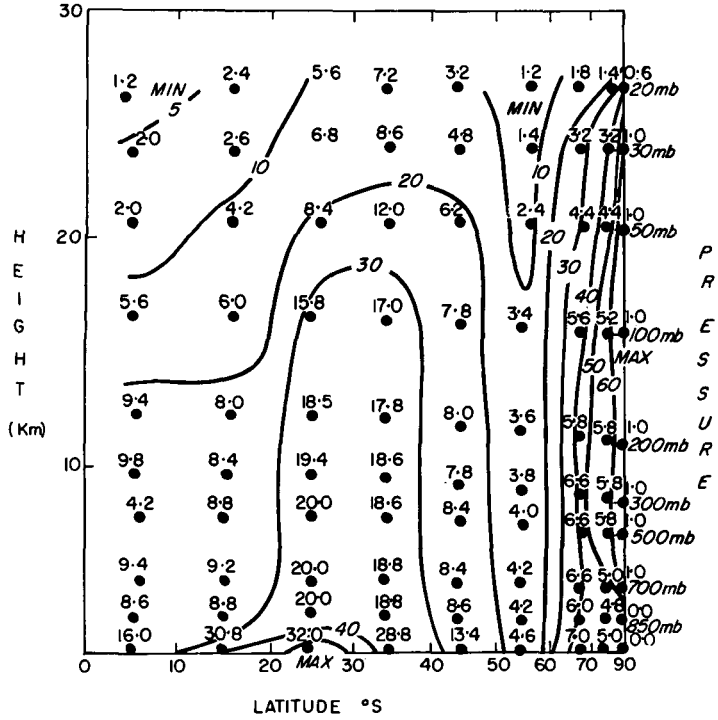

FIGURE 1.—Mean number of radiosonde soundings per day in each 10° latitude belt of the Southern Hemisphere. The isopleths show percentage coverage of the hemisphere as a function of latitude and height.

made available by the National Environmental Satellite Service aided in the analyses, in many cases enabling us to identify frontal systems, depressions, and an occasional jet stream. The intensity of systems and the relationship between pressure and temperature fields could only be qualitatively estimated. Special difficulty was experienced in the stratosphere, where data were both sparse and spatially and temporally inconsistent. No satisfactory method was found for resolving inconsistencies, other than conventional space- and time-smoothing techniques. Attempts to use regression techniques based on Northern Hemisphere investigations, such as those used by Finger et al. (1965) for vertical extrapolation of geopotential and temperature, proved fruitless. It was impossible to attempt synoptic analysis at the 10-mb level, and latitude-dependent mean values of geopotential and temperature had to be adopted. Mean humidity at the levels of low, medium, and high clouds was estimated in the data-free areas from the humidity-cloud relationships of Smagorinsky (1960) applied to the nephanalyses.

All data in the area poleward of latitude 20°S were then digitized on a polar stereographic grid of 1,977 points and checked by computer for vertical consistency of temperatures and height increments; implied superadiabatic lapse rates were adjusted to adiabatic values where detected. Finally, the data were subjected to the initialization procedures described by Smagorinsky et al. (1967) to obtain initial fields of wind components, temperature, and humidity and interpolated to the model grid of 5,025 points. In the course of these operations, as in the procedures mentioned above, temperature, geopotential, and humidity data equatorward of about 20°S were smoothly interpolated to a uniform value, equal to the mean value at latitude 20°S, in the equatorial zone.

Collecting all available data for the 5 days from their various sources and checking, plotting, analyzing, and digitizing these data were laborious tasks, requiring much of the time (9 mo) available for this aspect of the joint project. Thus, the desideratum of at least 15 days of analyzed data (the first for initial conditions and the remainder for verification of a 14-day forecast) was not achieved. Only 1000- and 500-mb height contours prepared by the International Antarctic Analysis Centre, Melbourne, Australia, were available for verification of the last 10 days of the forecast. These analyses covered the area poleward of latitude 30°S and all longitudes with the exception of 80°–130°W. The analyses were extended to latitude 20°S by reference to the available data, and the longitudinal gap in each case was filled subjectively by the customary forward and backward projection of systems from the analyzed areas.

3. THE MODEL AND THE COMPUTING PROCEDURE

The model used was the GFDL nine-level primitive-equation model described in essential detail by Smagorinsky et al. (1965) and Manabe et al. (1965). Application of this model to prediction experiments has been described by Smagorinsky et al. (1967) and Miyakoda et al. (1969). The methods used for representing the physical processes in the present model are described by Miyakoda et al. (1971*a*).

Briefly, the model includes: moist processes, as in Manabe et al. (1965), except that the moist convective adjustment is applied when the relative humidity is 80 percent or more; orography, smoothed to consistency with the grid; long- and short-wave radiation (where humidity, clouds, and ozone are based on Northern Hemisphere height-latitude mean values for October); constant (mean March) insolation; constant (mean March) sea-surface temperature; a water availability factor (over land), $D_W = E/E_{pot}$, which is the ratio of evaporation to potential evaporation computed from climatological precipitation data with the use of a procedure from Saltzman (1967); and prescribed albedo and snow cover. The sea-ice surface temperature was held constant at 268.5°K. Grid spacing is characterized as N40 on a polar sterographic projection (i.e., 40 grid intervals from Equator to pole) with resolution varying from 320 km at the pole to 160 km at the Equator. Horizontal diffusion is modeled as in Smagorinsky et al. (1965), except that Smagorinsky's horizontal mixing constant, k_0, has been reduced from 0.4 to 0.25 (Miyakoda et al. 1971*b*).

The initialization procedures (Smagorinsky et al. 1967) were applied to each of the five data sets, 0000 GMT on Mar. 1–5, 1965; the diagnostic procedures were applied to each day's data; and the results were averaged to give a 5-day mean picture of processes poleward of 20°S. These are expected to be valid within the limitations of the original analyses and the initialization procedures.

According to Gauntlett (1971), application of the balance equation results in some smoothing of the initial

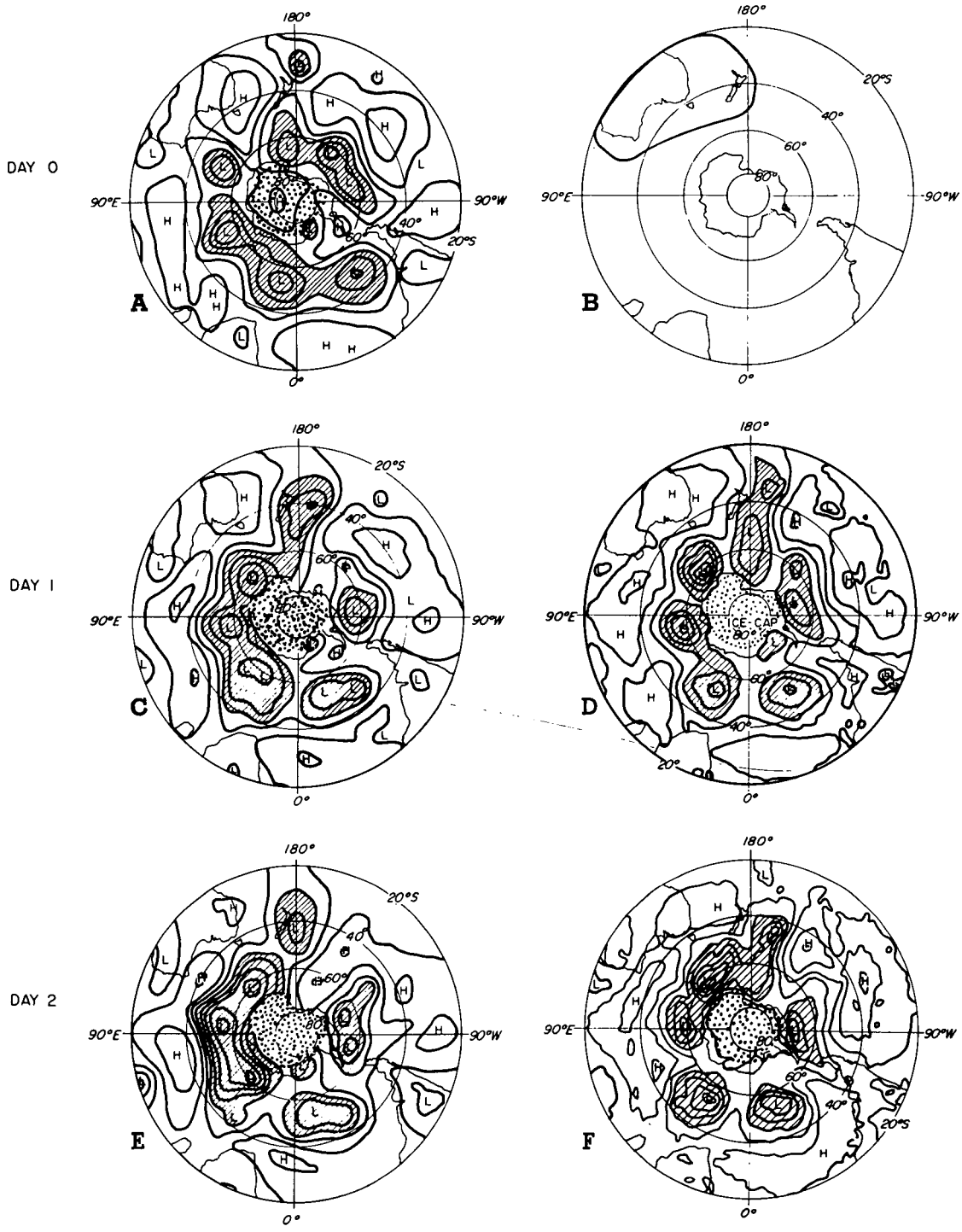

FIGURE 2.—Observed (A, C, E) and predicted (D, F) 1000-mb contours (60-m intervals), South Pole to latitude 20°S, for days 0–2. Negative areas are shaded. B delineates the Australasian sector referred to in section 4.

data, especially in the vicinity of the jet stream. Examination of the raw data suggests that flattening of the zonal wind profile in this way is minor in the present instance.

The ω-equation, used for computing vertical velocity and horizontal divergence, is based on the assumption of adiabatic, frictionless flow. It is to be expected, therefore, that divergence magnitudes in the boundary layer would be underestimated, as will those of vertical velocity at all levels, together with dependent quantities such as vertical eddy fluxes. The magnitude of ageostrophic wind components will also be underestimated in the boundary layer.

The prediction procedures of the GFDL model were applied to the initialized data for 0000 GMT on Mar. 1, 1965, to produce forecasts out to 14 days. The predicted fields were then subjected to statistical analysis by averaging various quantities at 12-hr intervals. A few of the diagnostic results so obtained are shown in figures 5 and 6.

4. VERIFICATION AND EVALUATION OF THE FORECASTS

The task of verification is complicated by the lack of reliable verifying data over much of the hemisphere.

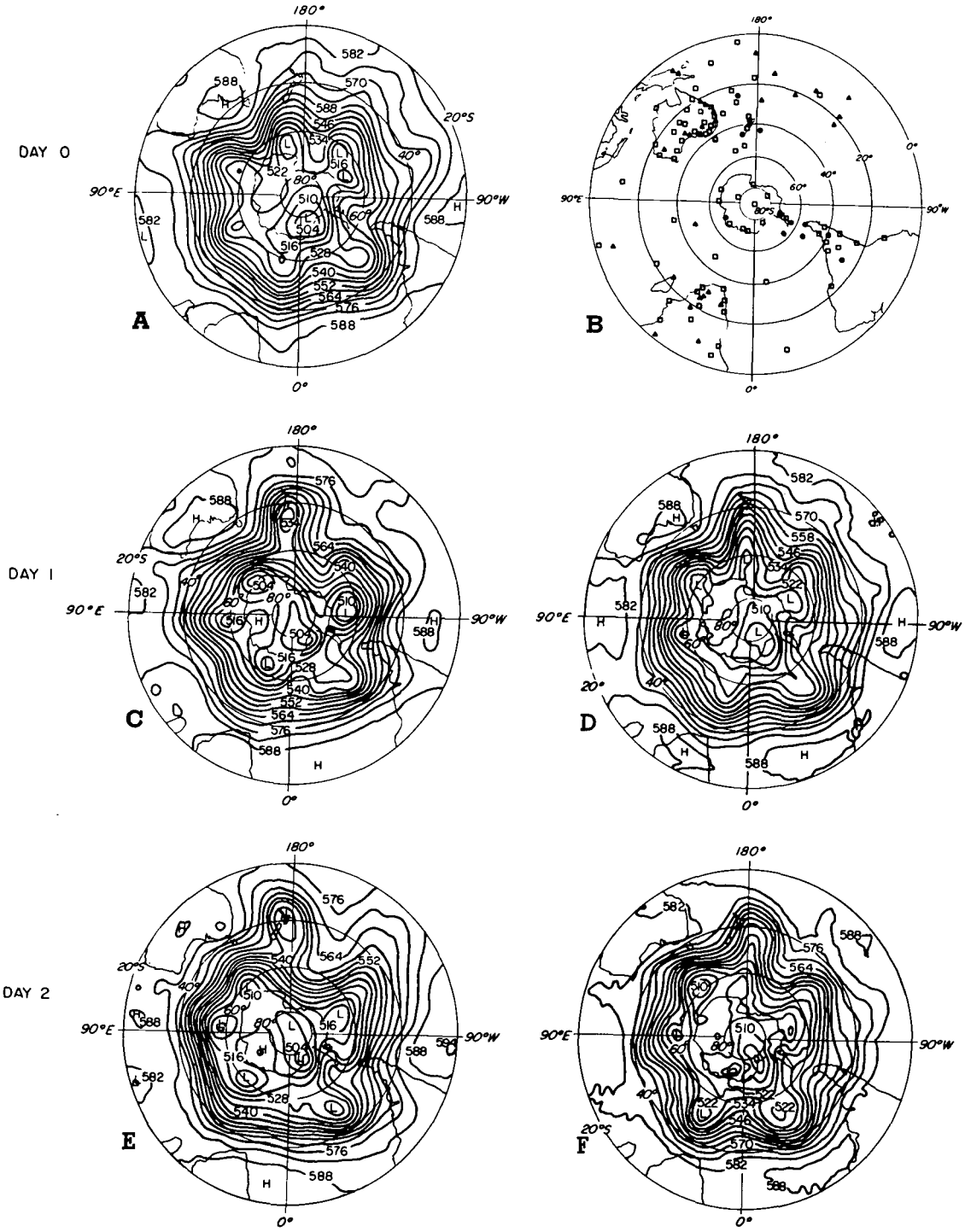

FIGURE 3.—Observed (A, C, E) and predicted (D, F) 500-mb contours (60-m intervals), South Pole to latitude 20°S, for days 0–2. B shows the location of wind (triangles), temperature (filled circles), and wind plus temperature (open squares) observations for day 0 at 500 mb.

Since the Australasian region is the only extensive area with good data coverage, we decided to verify the forecasts both on a hemispheric basis (2,453 gridpoints poleward of lat. 20°S) and a regional one (292 gridpoints in the Australasian region south of lat. 20°S, delineated in fig. 2B).

Hemispheric Verifications

Figures 2 and 3 show initial 1000- and 500-mb geopotential fields and forecast and "observed" fields for days 1 and 2 of the forecast. The hemispheric maps have been truncated at latitude 20°S, since few, if any, meaningful isopleths lie equatorward of that latitude. The 1000-mb height over Antarctica has been omitted because of its fictitious nature; it lies far below the elevated surface of the ice cap.

In general, the systems were predicted to progress a little too slowly eastward with the exception of the well-observed deep depression and trough to the east of New Zealand. The southeastward movement of this system was overpredicted by about 250 km/day. Some serious discrepancies are to be seen in the southeastern Pacific,

the worst region, datawise, in the hemisphere. In the vicinity of the Australian continent, agreement is good at both levels, although the predicted 500-mb trough south of the continent is lagging somewhat.

In figure 4A, the standard deviations of the errors in the forecasts of height of the 1000- and 500-mb surfaces are compared with those for a simple persistence prediction. With the exception of day 6, the skill at 500 mb remains positive throughout the 14 days, but no claim is made that the skill so indicated is useful beyond the first 2 days. At 1000 mb, the skill becomes and remains virtually zero at and after day 4.

Performance of Model in the Southern Hemisphere Versus Northern Hemisphere

The model should perform almost equally well in the two hemispheres, given the same data density and accuracy, although one might expect minor differences due to orography and the hitherto unexplored effect of a summer, as against a winter, situation. Thus, the differences in performance may generally be attributed to observational deficiencies in the Southern Hemisphere; these deficiencies affect both the quality of the forecast and of the verification.

A comparison of the performances (figs. 4B, 4C) reveals at once the general superiority of the Northern Hemisphere forecasts. Exceptions are day 1 at 1000 mb and the second week at 500 mb. Such a recovery in the second week has not been observed in Northern Hemisphere forecasts, and its occurrence in the first Southern Hemisphere case must be regarded as fortuitous.

The skill scores at 50 mb are not shown; these are very poor, as might be expected from the data availability. Correlations range from 0.3 to 0.6, and the skill score, V, is negative throughout the 4 days available for verification. (For definition of V, see caption to fig. 4.) Radok (1967) pointed out that correlation between predicted and observed changes will have a value of 0.5 if the covariances between observed and initial, observed and forecast, and initial and forecast fields are all equal (i.e., there is no skill). The value 0.5 broadly corresponds to the point where forecast errors are comparable with persistence. Thus, one should not accept correlation values as low as 0.5 as evidence of skill.

Some Statistical Properties of the Predictions

It is desirable to apply some kind of hemispheric check on the statistical properties of the forecasts to learn whether the model atmosphere behaves realistically in a statistical sense. In the present case, an overall check on the properties of the observed atmosphere is also needed.

An extensive range of diagnostic integral computations has been devised by GFDL. In the present case, we have the mean values of these integrals derived from the initialization procedures for each of the 5 days, together with averages estimated from the raw data, equatorward of 20°S. These 5 days of data, displaying fairly satisfactory

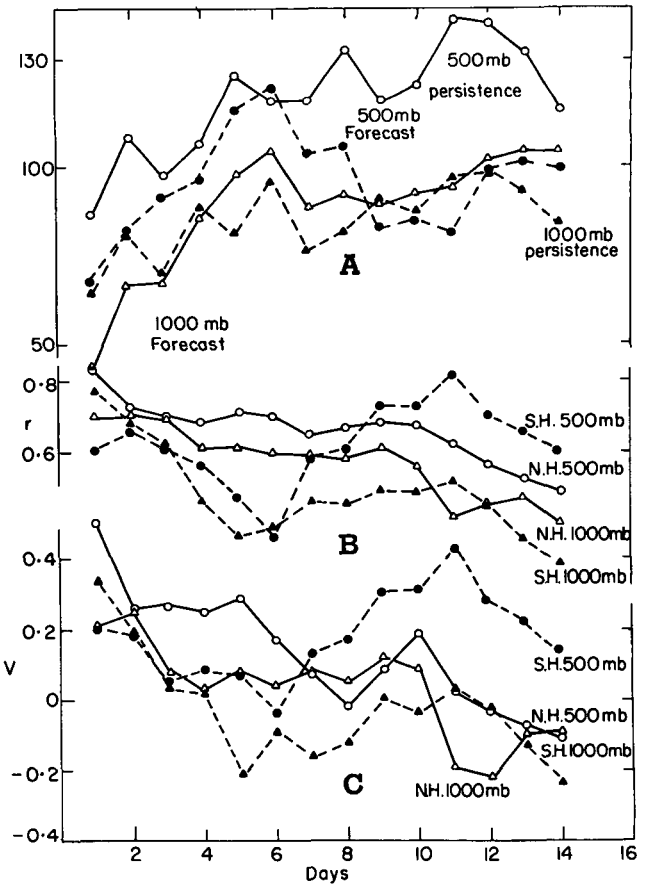

FIGURE 4.—(A) standard deviation of model forecast and persistence height errors (m) at 1000 and 500 mb for the hemisphere south of 20°S, (B) correlation between observed and predicted height changes at 100 and 500 mb for the hemisphere south of 20°S compared with similar correlations for Northern Hemisphere forecasts (Miyakoda et al. 1969), and (C) skill score [$V = (\sigma_p - \sigma_f)/\sigma_p$] where σ_p and σ_f are standard deviation of persistence and forecast errors, respectively, for 1000 and 500 mb compared with the score for Northern Hemisphere forecasts.

statistical stationarity, may serve as observed values with which to compare similarly computed forecast values over the 14 days of the experiment. For this purpose, results from days 4 to 14 have been averaged. To limit the averaging to nearly stationary conditions, we have omitted the first 3 days when some of the space-mean properties, for example, meridional circulation, were changing rapidly. Clearly, only the statistics of long-period forecasts, such as in the present case, can be compared with those for the observed atmosphere in this manner. Some of the differences between the observed and predicted statistics may be related to the fact that different periods have been treated, but in most cases this is not true. Something of value can be learned from the comparison.

The integral properties chosen for comparison are shown in figures 5 and 6. As was expected, observed and predicted streamlines (fig. 5A) differ considerably, due, at least in part, to the deficiencies of the ω-equation that affect the observed but not the predicted field of flow. Nevertheless, there is qualitative agreement on the two main circulation cells and on the equatorward flow in the middle stratosphere (highest model level), although the

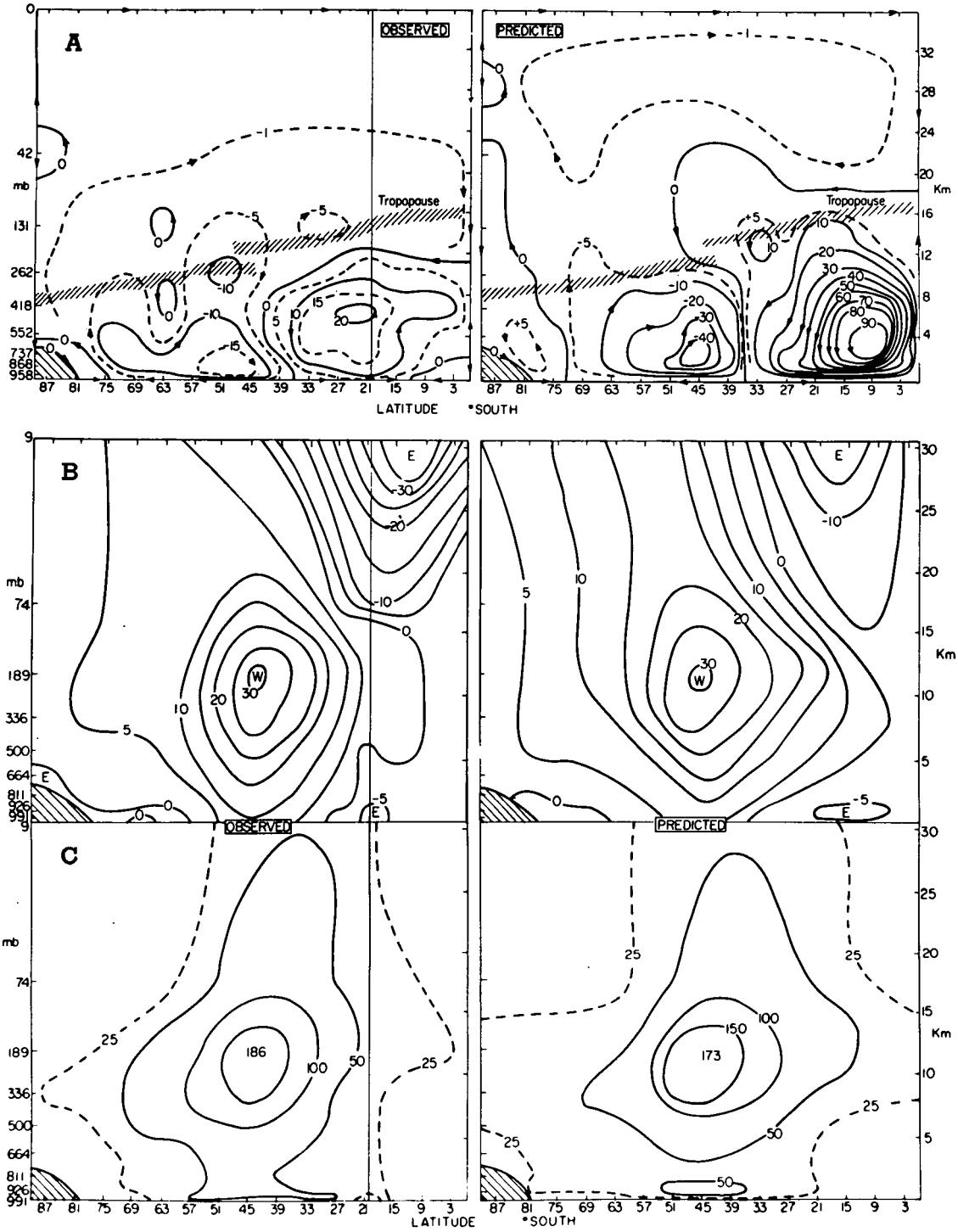

FIGURE 5.—(A) observed and predicted streamlines (10^{12} g/s) of the meridional circulation, (B) observed and predicted mean zonal wind speed (m/s), and (C) observed and predicted eddy kinetic energy $(\overline{u'^2} + \overline{v'^2})/2$ in $m^2 \cdot s^{-2}$ where u' and v' are departures from zonal means and the bar indicates a space-mean. The vertical line at latitude 20°S indicates the equatorward limit of the observed data used in initialization. Equatorward of this line, in (B) and (C), observed quantities are derived from raw data rather than from the initialization procedure.

polar meridional circulation cell is almost missing from the observed streamlines. The three cells computed by the model are in good qualitative agreement with those of Newell et al. (1970) for autumn, although they are somewhat stronger. Central values of the stream function are about 95 and -43×10^{12} g/s in the predicted, compared with 50 and -10×10^{12} g/s in Newell's analysis, for the Hadley and Ferrel cells, respectively.

The main features of the mean field of zonal wind (fig. 5B) were reproduced well. However, the westerly jet is predicted slightly poleward of its observed position, and the predicted easterly jet in the tropical stratosphere is much weaker than observed. The behavior of the model in low latitudes may be seriously affected by the equatorial wall, while the observed wind must be treated with reserve. Sadler's analysis (Miyakoda et al. 1971*a*, fig. 2) of the

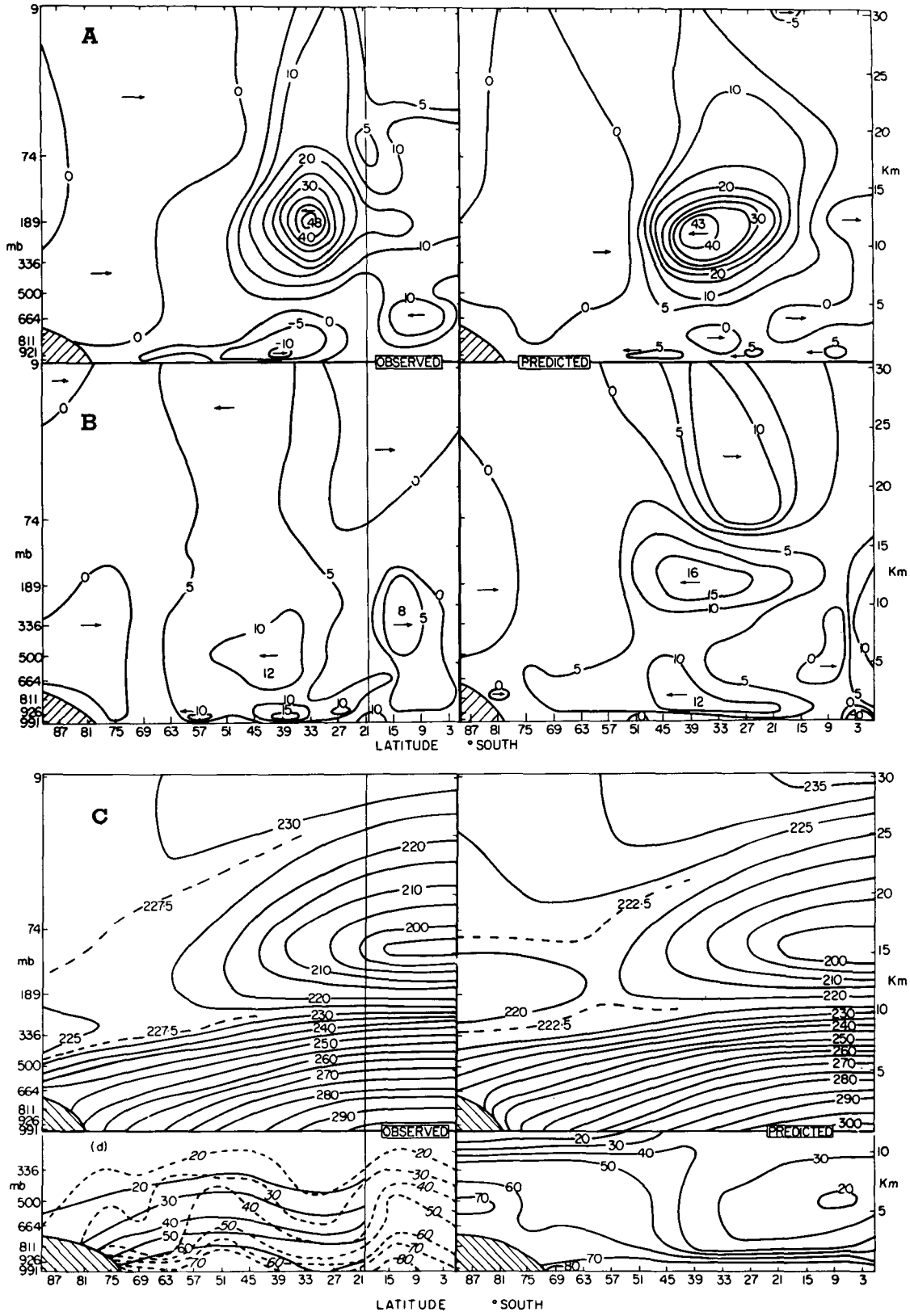

FIGURE 6.—(A) observed and predicted values of the quantity $2\pi R^2 \cos^3\phi \, \overline{v'u'}$ (10^{22} cm^4 · s^{-2}) where R is earth radius and ϕ is latitude, (B) observed and predicted values of the quantity $2\pi R \cos\phi \, c_p \, \overline{v'T'}$ (10^{18} cm^4 · s^{-3}) where T' is departure from zonal mean temperature and c_p is specific heat, (C) observed and predicted mean temperature (°K) [note that, equatorward of 20°S, quantities in (A)–(C) are estimated from raw radiosonde data], and (D) observed and predicted values of mean relative humidity (percent). Full lines for observed humidity are derived from initialization; broken lines are from the raw radiosonde data.

stratospheric easterlies differs from the present one in locating the maximum at the Equator. Ours, however, agrees well with that of Newell et al. (1970) for the southern summer. Another feature worthy of comment is the previously noted tendency for energy from the westerly jet to "leak" upward into the stratosphere; the

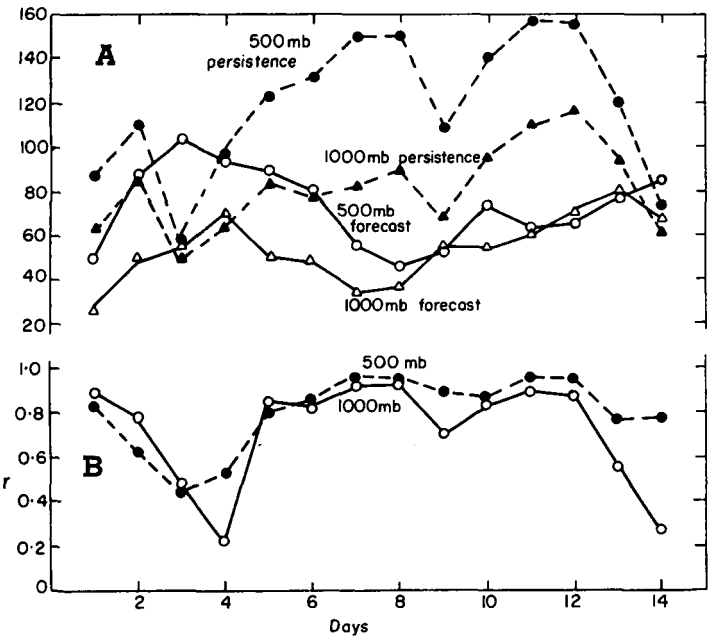

FIGURE 7.—(A) standard deviation of height errors (m) at 1000 and 500 mb for Australasia south of 20°S, with persistence errors, and (B) correlations between observed and predicted height changes at 1000 and 500 mb for Australasia south of 20°S.

observed mean westerly wind maximum of 5.8 m/s at level 1 ($\approx$9 mb) is magnified in the forecasts to 18.1 m/s.

Correspondence between predicted and observed values of meridional transport of angular momentum (fig. 6A) is not good, but, in view of the observational difficulties, it may be classified as acceptable. Both are in reasonable accord with Newell et al. (1970) and show a middle-latitude maximum of poleward transport of similar magnitude, although the predicted maximum is displaced somewhat toward the south. Both the observed and predicted patterns show a high-latitude equatorward flux, but the predicted maximum is larger than the observed (3.2×10^{22} compared with 1.9×10^{22} cm$^4\cdot$s^{-2}) and is shifted equatorward. Both show a region of equatorward flux (much larger in the observed case) at low levels beneath the poleward maximum. Such an equatorward flux was actually observed in the boundary layer during the Wangara experiment (Clarke et al. 1971), extending over 40 days at latitude 34.5°S. If the value found is representative of its latitude, the flux at 350 m above the ground would be 1.7×10^{23} cm$^4\cdot$s^{-2} toward the Equator.

Figure 6B presents observed and predicted meridional heat fluxes that may be compared with Robinson's (1970) annual distribution and the summer distributions of Newell et al. (1970). Because of the difficulty of matching temperature and geopotential in a realistic way in the course of estimating fields from satellite data, there are significant discrepancies. In both patterns, however, there is a broad midlatitude band of poleward flux with a maximum of $12\text{–}16\times10^{18}$ cm$^4\cdot$s^{-3} (cf. Robinson's mean annual value of 24×10^{18}) and a high-latitude and a low-latitude band of equatorward flux. The observed fluxes in the stratosphere bear little resemblance to the predicted ones, but observational difficulties here are overwhelming.

Figure 6C compares observed and predicted temperatures. Prediction errors are greatest near the pole (i.e., predicted temperatures are too low at all levels, reaching -8.3°K at $\approx$189 mb). In general, levels at and above 500 mb are too cold (areal mean temperature deficit reaching 2.1°K at $\approx$189 mb), and the lower troposphere is too warm (max. error 0.9°K at $\approx$926 mb).

The relative humidity comparison of figure 6D reveals some rather striking dissimilarities. Observed humidity is represented by two sets of isopleths, one (dashed lines) based entirely on raw station data, averaged by 10° latitude belts, and the other (solid line), from the initialization procedures. Miyakoda et al. (1971*a*) suggest that insufficient moisture is predicted in the Tropics because the equatorial wall prevents the cross-equatorial flow of moisture from the winter hemisphere to the summer hemisphere, which is a feature of the real Tropics.

Verification in the Australasian Sector

Regional verification is based on too small an areal sample to be used as a test of general capability of the model; but it is a much more satisfactory exercise in that one may have confidence in the observed data. For rainfall verification, there is at present little alternative but to check on a regional basis.

Figures 7A and 7B show the standard deviation of the geopotential error and correlations, respectively, between observed and predicted height changes for the Australasian sector. The performance of the model in this series is somewhat better over the Australasian sector than elsewhere at both 1000 and 500 mb despite the fact that activity, as judged by surface pressure variance and rainfall, was above normal during the period. Also, for the first 2 days, the 1000-mb level, which in general is more difficult to predict, appears to verify better than 500 mb, possibly reflecting the effect of a better data network at the lower level.

Figure 8 shows observed and predicted maps of the 1000- and 500-mb heights on day 7 for the Australasian sector. One sees at once that the high skill score results only from a correct placement of the main trough; the details are not correctly predicted, nor is the rain well foreshadowed.

Figure 9 presents Hovmöller diagrams of the 1000- and 500-mb predicted and observed geopotential, averaged between latitudes 35° and 45°S, for the Australasian sector (115°E–170°W). After the first few days, during which the model failed to predict the lack of movement of the depression east of New Zealand, the course of the trough and ridge pattern is fairly well reproduced, albeit with diminished amplitude. A noteworthy feature is the failure to predict the rearward redevelopment of the trough over southern Australia on day 9.

Since the model computes rainfall, it is of considerable interest to check how well the daily accumulation of rainfall compares with that predicted. For this purpose, it is desirable to average many rainfall recordings in the area represented by each gridpoint of the computational mesh. The 1,660 regularly reporting precipitation stations in

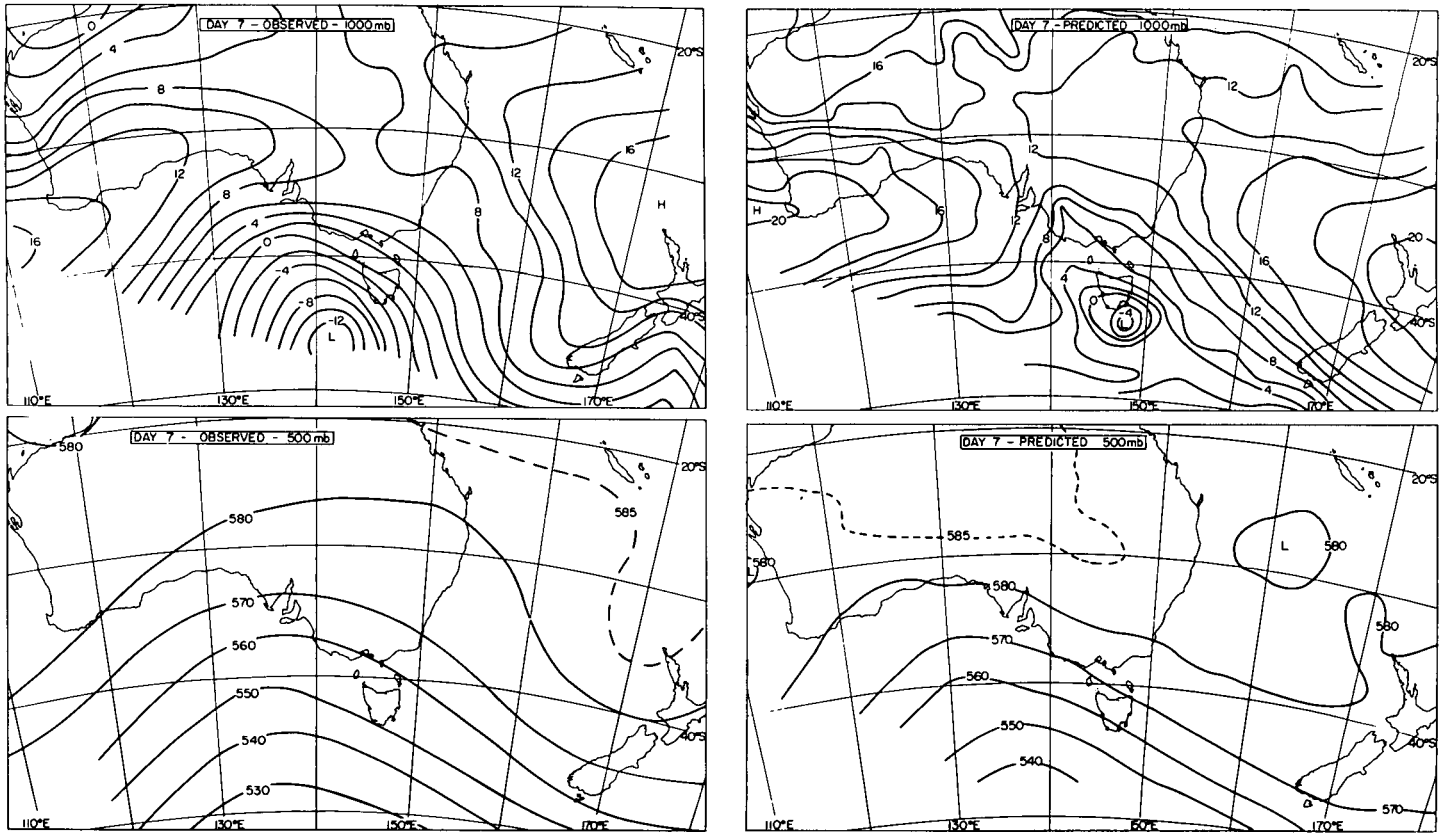

FIGURE 8.—Observed and predicted constant pressure [contours in dekameters (dam)] for day 7 in the Australasian sector.

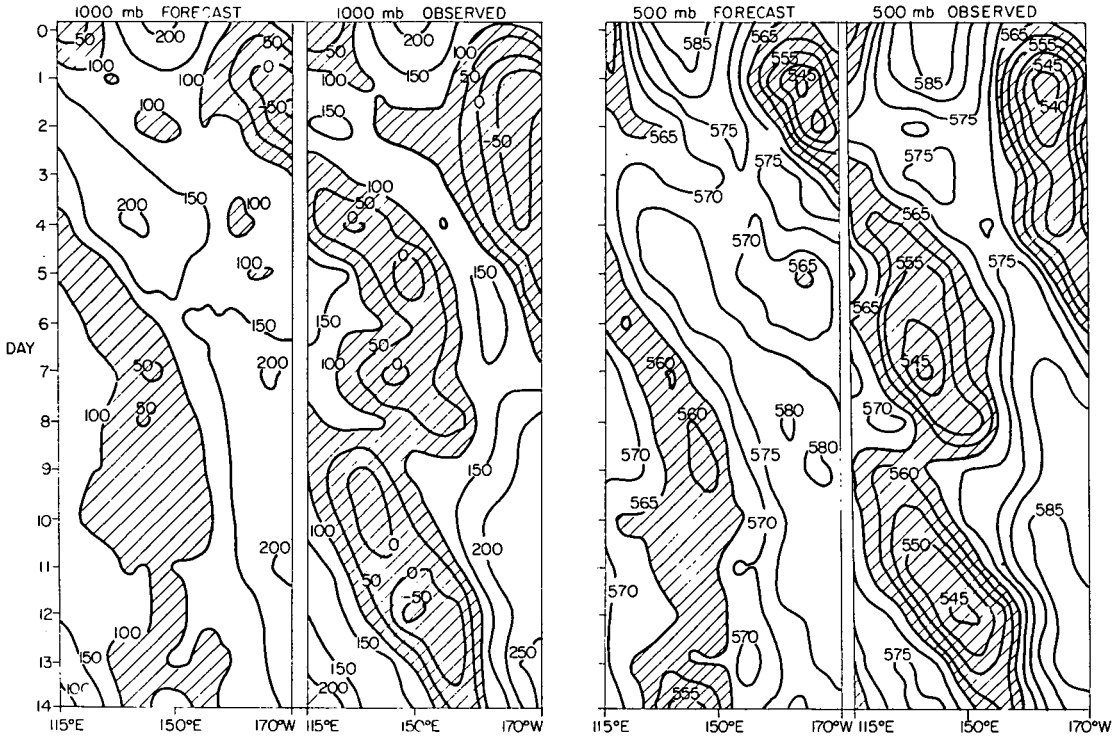

FIGURE 9.—Hovmöller diagrams showing observed and predicted mean height of the 1000-mb surface (m) and the 500-mb surface (dam) between latitudes 35° and 45°S as a function of longitude and time in the Australasian sector (115°E–170°W).

the mainland network of the Commonwealth Bureau of Meteorology are very unevenly distributed; of the 178 gridpoints falling on the Australian mainland, 37 had no rain stations at all, while 32 of the remainder had only one. Only 53 had more than five rain stations. We decided to use all gridpoints having at least one rain station, averaging stations where there were more than one, for comparison with predicted precipitation values. It should also

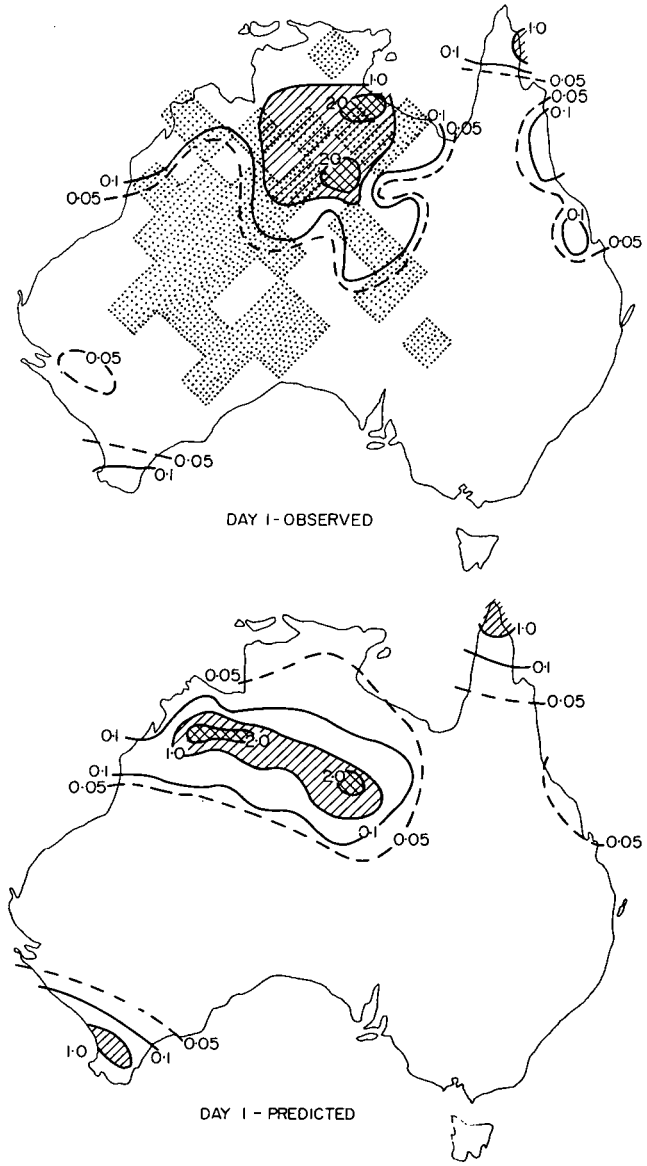

FIGURE 10.—Observed and predicted accumulated rainfall (in.) at day 1 over the Australian continent. The grid squares with no data are indicated by shading.

be noted that Australian rain gages are read at 0900 LST, which implies a discrepancy of from 1 to 3 hr in various parts of the continent from the time of the predicted accumulations at 0000 GMT.

Figure 10 shows accumulated predicted and average observed rainfall at the 141 gridpoints for which data are available on day 1. One can see that a fair measure of agreement has been achieved despite the unsatisfactory method of initialization north of latitude 20°S where the bulk of the precipitation occurs. On subsequent days, the agreement is much less marked, and the application of statistical methods of detecting skill is required. The following two methods have been applied:

1. The first method consists of correlating predicted and observed rainfalls at each of the 141 gridpoints. To reduce the marked skewness of the distributions, we correlated the cube root of the rainfall amounts after rounding to the nearest 0.01 in. (0.254 mm). The results for each of the 14 days of the forecast are shown in curve I of figure 11. Predictions made with the global model (Miyakoda et al. 1971a), which from most points of view verified lower than the hemispheric model, yielded higher overall rainfall correlations over Australia (0.35 vs. 0.19 for the 14-day average, with 0.66 and 0.57 on the first 2 days). This might be expected from the more realistic initialization in the Tropics.

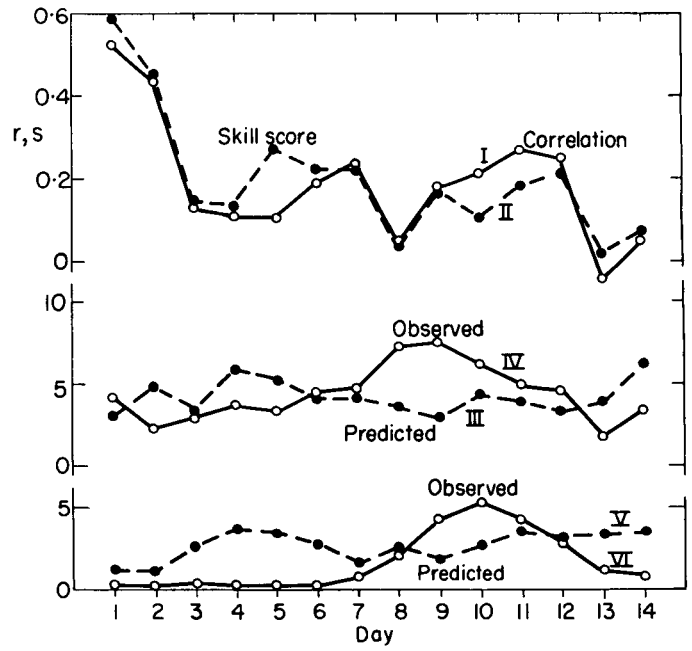

FIGURE 11.—Rainfall verification over the Australian continent: (I) correlations between cube root of predicted and observed rainfall, (II) Wallen's skill score calculated on a rain-no rain basis, (III) mean predicted rainfall in mm/day (Australia), (IV) mean observed rainfall (Australia), (V) mean predicted rainfall (Australia south of 20°S), and (VI) mean observed rainfall (Australia south of lat. 20°S).

2. If the precipitation forecasts are regarded as hit or miss prediction of rain or no rain, Wallen's method (Bleeker 1946) of verification can be applied. This has been used successfully to test the value of long-range forecasting systems. To allow for the tendency of the model to produce small values of precipitation over large areas, we regarded only predicted precipitation of more than 1 mm as a forecast of rain, while observed rainfall of 0.25 mm or more was regarded as constituting a rain day. The skill score achieved by this system is shown in curve II of figure 11 and is seen to agree closely with that indicated by the correlations. For most practical purposes, the useful skill is confined to the first 2 days.

To illustrate the performance of the model in Australia's rather extreme summer conditions (the gridpoints for testing rainfall range from lat. 11° to 41°S), we add curves III–VI in figure 11. They represent areal mean predicted and observed precipitation over (1) the Australian continent (141 points) and (2) that portion of the continent (100 points) south of latitude 20°S. Curves III and IV (14-day means are 4.24 and 4.36 mm/day, respectively) show that, overall, the predictions yielded results very close to those observed. On the other hand, curves V and VI show that too much rain is predicted for the dry southern part of the continent (14-day predicted and observed means are 2.70 and 1.63 mm/day). Areal averaging showed that, for that part of the continent covered by our data, March normal rainfall is much less than that measured over this particular 14 days (in the ratio 1.73:4.36 for the whole continent and 1.42:1.63 for that part south of lat. 20°S).

As another test of the summertime performance of the model, the forecast results were checked for evidence of the monsoon, which manifests itself in anomalously high temperatures and low pressures in the lower levels of the troposphere, and a low-level mean cyclonic circulation with inflow. No such evidence was found in the forecast fields. For example, mean inflow at the coast was 22 and 8 cm/s at levels 8 ($\approx$926 mb) and 9 ($\approx$991 mb) compared to an observed value of 120 cm/s at 300–500 m. The mean temperature excess over the continent at level 9 was 0.5°K, compared with 3.5°K for the mean March screen temperature. These defects, and possibly the excessive rainfall computed south of latitude 20°S, are believed to be due largely to the unrealistic values adopted for $D_w = E/E_{pot}$ over the dry Australian interior. South of latitude 20°S, the water availability factor ranged from 0.3 to 0.8. The resulting evaporation computed over the driest part of the continent was little less than that over the neighboring oceans.

With the use of Budyko's (1960) values for mean net radiation in March, and with E, the evaporation rate, assumed equal to the mean rainfall for the area south of latitude 20°S, we found that the Bowen ratio, $H/\mathscr{L}E$ (H is sensible heat flux at the surface, $\mathscr{L}$ is the latent heat of vaporization for water), should have a mean value of about 2, as opposed to that of 0.08 computed from the forecasts. Thus, there appears to be a need for a formulation of E/E_{pot} in terms of water substance in the soil; that is, one that will not imply an evaporation of nonexistent soil moisture.

The Antarctic Circulation

A further test of the model is its ability to reproduce the well-known vertical circulation over Antarctica (Rubin and Weyant 1963, Berson 1966) and its katabatic winds (Ball 1957). Rubin and Weyant calculated the mean outflow at standard pressure levels. At the lowest level used (850 mb), the mean outflow for March was 1.4 m/s, decreasing to zero a little above 700 mb. Berson computed the mean outflow for a 40-day period in spring to be 3.3 m/s at 980 mb and 2.6 m/s at 940 mb, decaying to nearly zero at 700 mb.

This outflow and the corresponding higher level inflow and interior descent are modeled with some success, as may be seen from the predicted streamlines (fig. 5A). Mean vertical velocities were predicted to be about -0.3 cm/s in areas poleward of latitude 80°S at the 500- to 600-mb level decreasing with height and becoming positive above 100 mb. In the lower levels, this agrees well with the vertical velocities deduced by Berson and by Rubin and Weyant.

An examination of the model outflow values, referred to Antarctic topography, shows that at level 9 (representing roughly the lowest 300 m) the mean outflow is 3.5 m/s at the coast, decreasing to 1.8 m/s at the 1800-m contour, in good agreement with Berson's value. However, no mean outflow is predicted at higher levels around the coast. The computed depth of the anticyclonic circulation around the continent is a little above 1000 m, compared with an observed spring value of nearly 3000 m. Thus, the katabatic outflow with anticyclonic circulation is reproduced in the model, but its depth is probably underestimated.

5. CONCLUSIONS

The results of this experiment suggest that, despite the present serious lack of suitable data in the Southern Hemisphere, hemispheric forecasts useful for 2 or 3 days can be made with the GFDL model. During this period, skill was found to decline with height, probably reflecting the superior surface data coverage.

From the first few days, the model performed generally worse in the Southern Hemisphere than in the Northern Hemisphere, as might be expected from the data availability. Nevertheless, at 1000 mb where data are more plentiful, the first 2 days' results were comparable with those for the Northern Hemisphere.

Over the Australasian sector, the largest region represented by anything approaching an acceptable data coverage, the model performance in the first 2 days was superior in almost every respect to that in the rest of the hemisphere. Its performance was sufficient to raise hopes that weather forecasting (including rainfall) in this region, for 2 days and perhaps more, can be markedly improved. This conclusion is supported by recent results with a modified version of the same model (Gauntlett and Hincksman 1971).

A disappointing feature of the present series was the failure to predict the virtual lack of movement of the deep New Zealand depression for the first 4 days. But for this failure, skill scores may well have been higher on the third and fourth days in the Australian area.

One should not read too much into the high skill scores indicated for the second week of the forecast at 500 mb for the hemispheric prediction and at both 500 and 1000 mb over Australia. It may be significant that there is little, if any, response to this skill in the Australian rainfall predictions. The evidence of skill in the Australasian region, nevertheless, excites speculation that a "data oasis" may have some advantages in medium-range predictability.

The summer monsoon over Australia is not well reproduced by the model, due apparently to a weakness in modeling evaporation. Greater success in modeling the circulation was achieved over Antarctica.

ACKNOWLEDGMENTS

The authors owe a great debt of gratitude to other members of GFDL, especially J. Smagorinsky, who made these experiments possible; K. Miyakoda, who contributed much help and guidance; and G. D. Hembree, whose help in collection, preparation, and initialization of the data was indispensable. M. L. Neff, L. W. Reed, I. Shulman, and T. L. Mauk also provided much skilled assistance in programming and data handling problems.

REFERENCES

Ball, F. K., "The Katabatic Winds of Adélie Land and King George V Land," *Tellus*, Vol. 9, No. 2, Stockholm, Sweden, May **1957**, pp. 201–208.

Baumhefner, David P., "Global Real-Data Forecasts With the NCAR Two-Layer General Circulation Model," *Monthly Weather Review*, Vol. 98, No. 2, Feb. **1970**, pp. 92–99.

Berson, F. A., "The Mass and Heat Budgets of the Atmosphere Over the Antarctic Plateau (With Particular Reference to Spring)," *Technical Report* No. 6, International Antarctic Meteorological Research Centre, Commonwealth Bureau of Meteorology, Melbourne, Australia, **1966**, 51 pp.

Bleeker, Wouter, "The Verification of Weather Forecasts," *Mededeelingen en Verhandelingen*, Ser. B, Deel 1 No. 2, Meteorologisch Instituut, The Hague, Netherlands, **1946**, 23 pp.

Budyko, M. I. (Editor), "Atlas of Thermal Balance," *Publication* 19, Arctic Meteorology Research Group, McGill University, Montreal, Quebec, Canada, Feb. **1960**, 35 pp. (translation of *Atlas Teplovago Balansa*, Glavnaia Geofizcheskaia Observatoriia, Leningrad, U.S.S.R., 1955, 41 pp.).

Clarke, R. H., "Southern Ocean Analysis," *Australian Meteorological Magazine* No. 5, Commonwealth Bureau of Meteorology, Melbourne, Australia, Jan. **1954**, pp. 33–54.

Clarke, R. H., Dyer, A. J., Brook, R. R., Reid, D. G., and Troup, A. J., "The Wangara Experiment: Boundary Layer Data," *C.S.I.R.O. Technical Paper* No. 19, Commonwealth Scientific and Industrial Research Organization, Melbourne, Australia, **1971**, 362 pp.

Finger, F. G., Woolf, H. M., and Anderson, C. E., "A Method for Objective Analysis of Stratospheric Constant-Pressure Charts," *Monthly Weather Review*, Vol. 93, No. 10, Oct. **1965**, pp. 619–638.

Gauntlett, D. J., "Initialisation Experiments in the Southern Hemisphere," *Internal Scientific Report* No. 7, Commonwealth Meteorology Research Centre, Melbourne, Australia, **1971**, 15 pp.

Gauntlett, D. J., and Hincksman, D. R., "A Six-Level Primitive Equation Model Suitable for Extended Operational Prediction in the Southern Hemisphere," *Journal of Applied Meteorology*, Vol. 10, No. 4, Aug. **1971**, pp. 613–625.

Jenssen, D., and Radok, Uwe, "An Experiment in the Numerical Prediction of Rain," Papers from the Seminar on Rain, Sydney, Australia, August 1960, Commonwealth Bureau of Meteorology, Melbourne, **1960**, 12 pp.

Manabe, Syukuro, Smagorinsky, Joseph, and Strickler, Robert F., "Simulated Climatology of a General Circulation Model With a Hydrologic Cycle," *Monthly Weather Review*, Vol. 93, No. 12, Dec. **1965**, pp. 769–798.

Miyakoda, K., Moyer, R. W., Stambler, H., Clarke, R. H. and Strickler, R. F., "A Prediction Experiment With a Global Model Using the Kurihara Grid," *Journal of the Meteorological Society of Japan*, Vol. 49, Special Issue, Tokyo, Dec. **1971***a*, pp. 1–16.

Miyakoda, K., Smagorinsky, J., Strickler, R. F., and Hembree, G. D., "Experimental Extended Predictions With a Nine-Level Hemispheric Model," *Monthly Weather Review*, Vol. 97, No. 1, Jan. **1969**, pp. 1–76.

Miyakoda, K., Strickler, R. F., Nappo, C. J., Baker, P. L., and Hembree, G. D., "The Effect of Horizontal Grid Resolution in an Atmospheric Circulation Model," *Journal of the Atmospheric Sciences*, Vol. 28 No. 4, May **1971***b*, pp. 481–499.

Newell, R. E., Vincent, D. G., Dopplick, T. G., and Ferruza, P., "The Energy Balance of the Atmosphere," *The Global Circulation of the Atmosphere*, Royal Meteorological Society, London, England, **1970**, pp. 42–90.

Radok, U., University of Melbourne, Australia, July **1967** (personal communication).

Robinson, John Ball, Jr., "Meridional Eddy Flux of Enthalpy in the Southern Hemisphere During the IGY," *Pure and Applied Geophysics*, Vol. 80, Basel, Switzerland, **1970**, pp. 319–334.

Rubin, Morton J., and Weyant, William S., "The Mass and Heat Budget of the Antarctic Atmosphere," *Monthly Weather Review*, Vol. 91, Nos. 10–12, Oct.–Dec. **1963**, pp. 487–493.

Saltzman, B., "On the Theory of the Mean Temperature of the Earth's Surface," *Tellus*, Vol. 19, No. 2, Stockholm, Sweden, May **1967**, pp. 219–229.

Smagorinsky, Joseph, "On the Dynamical Prediction of Large-Scale Condensation by Numerical Methods," *Geophysical Monograph* No. 5, American Geophysical Union, Washington, D.C., **1960**, pp. 71–78.

Smagorinsky, Joseph, Manabe, Syukuro, and Holloway, J. Leith, Jr., "Numerical Results From a Nine-Level General Circulation Model of the Atmosphere," *Monthly Weather Reiew*, Vol. 93, No. 12, Dec. **1965**, pp. 727–768.

Smagorinsky, J., Strickler, R. F., Sangster, W. E., Manabe, S., Holloway, J. L., and Hembree, G. D., "Prediction Experiments With a General Circulation Model," *Proceedings of the Second International Symposium on Dynamics of Large-Scale Processes in the Atmosphere, Moscow, U.S.S.R., June **23–30**, **1965***, Izdatelstvo "Nauka," Moscow, **1967**, pp. 70–134.

Staff, NMC (National Meteorological Center), Weather Bureau, ESSA, "A Global Numerical Prediction for Apollo 13," *Bulletin of the American Meteorological Society*, Vol. 51, No. 7, July **1970**, pp. 594–601.

Streten, N. A., "A Note on the Frequency of Closed Circulations Between 50°S and 70°S in Summer," *Australian Meteorological Magazine*, Vol. 17, No. 4, Melbourne, Dec. **1969**, pp. 228–234.

Taljaard, J. J., "Development, Distribution and Movement of Cyclones and Anticyclones in the Southern Hemisphere During the IGY," *Journal of Applied Meteorology*, Vol. 6, No. 6, Dec. **1967**, pp. 973–987.

[*Received October 26, 1971; revised March 3, 1972*]